NOAA Technical Report NOS CS 39

EVALUATING THE BENEFIT AND COST OF ASSIMILATING SATELLITE SEA SURFACE TEMPERATURE INTO THE NOAA CHESAPEAKE BAY OPERATIONAL FORECAST SYSTEM USING 4DVAR AND LETKF

Silver Spring, Maryland
January 2020

noaa National Oceanic and Atmospheric Administration

U.S. DEPARTMENT OF COMMERCE
National Ocean Service
Coast Survey Development Laboratory

Office of Coast Survey
National Ocean Service
National Oceanic and Atmospheric Administration
U.S. Department of Commerce

The Office of Coast Survey (OCS) is the Nation's only official chartmaker. As the oldest United States scientific organization, dating from 1807, this office has a long history. Today it promotes safe navigation by managing the National Oceanic and Atmospheric Administration's (NOAA) nautical chart and oceanographic data collection and information programs.

There are four components of OCS:

The Coast Survey Development Laboratory develops new and efficient techniques to accomplish Coast Survey missions and to produce new and improved products and services for the maritime community and other coastal users.

The Marine Chart Division acquires marine navigational data to construct and maintain nautical charts, Coast Pilots, and related marine products for the United States.

The Hydrographic Surveys Division directs programs for ship and shore-based hydrographic survey units and conducts general hydrographic survey operations.

The Navigational Services Division is the focal point for Coast Survey customer service activities, concentrating predominately on charting issues, fast-response hydrographic surveys, and Coast Pilot updates.

NOAA Technical Report NOS CS 39

EVALUATING THE BENEFIT AND COST OF ASSIMILATING SATELLITE SEA SURFACE TEMPERATURE INTO THE NOAA CHESAPEAKE BAY OPERATIONAL FORECAST SYSTEM USING 4DVAR AND LETKF

Matthew J. Hoffman[1], Bin Zhang[2], Lyon Lanerolle[3,4], and Christopher W. Brown[2,5]

1 School of Mathematical Sciences, Rochester Institute of Technology, Rochester, NY
2 Earth System Science Interdisciplinary Center, University of Maryland, College Park, MD
3 Coast Survey Development Laboratory, National Oceanic and Atmospheric Administration, Silver Spring, MD
4 Department of Math and Sciences, Kapiolani Community College, Honolulu, HI
5 Center for Satellite Applications and Research, National Oceanic and Atmospheric Administration, College Park, MD

Corresponding Author: Christopher Brown, 5825 University Research Court, Suite 4001, College Park, MD 20740; email: Christopher.W.Brown@noaa.gov; tel: 301-405-8031

January 2020

noaa **National Oceanic and Atmospheric Administratio**

U. S. DEPARTMENT OF COMMERCE **Wilbur Ross, Secretary**	**National Oceanic and Atmospheric Administration** **Dr. Neil Jacobs, Acting Under Secretary**	**National Ocean Service** **Nicole LeBoeuf, Acting Assistant Administrator**

Office of Coast Survey **Capt. Richard Brennan** **Acting Director**	**Coast Survey Development Laboratory** **Dr. Shachak Pe'eri** **Division Chief**

NOTICE

Mention of a commercial company or product does not constitute an endorsement by NOAA. Use for publicity or advertising purposes of information from this publication concerning proprietary products or the tests of such products is not authorized.

TABLE OF CONTENTS

LIST OF TABLES

LIST OF FIGURES

ABSTRACT

The National Oceanic and Atmospheric Administration (NOAA) presently does not assimilate observations into the coastal ocean Operational Forecast System (OFS). We conducted a preliminary assessment of the skill and computational cost/effort of two popular data assimilation techniques – Four-Dimensional Variational (4DVAR) and the Local Ensemble Transform Kalman Filter (LETKF) – in assimilating satellite-derived, sea-surface temperature (SST) into the NOAA's Chesapeake Bay Operational Forecast System (CBOFS) with the intention of improving nowcasts and forecasts. Sea-surface temperatures from NOAA's Visible Infrared Imager Radiometer Suite (VIIRS) onboard the Suomi National Polar Orbiting Partnership (SNPP) are used to correct the temperature field in CBOFS and the results are compared to independent temperature observations from buoys and vertical CTD profiles. Both 4DVAR and LETKF provide improvement in temperature nowcasts and forecasts over the free running model, reducing their errors by 1°C or more, with improvements not only in the surface but throughout the water column. The results of this study demonstrate that data assimilation of satellite retrievals of SST can increase skill in model predictions in estuarine waters and provide information that will aid NOAA in deciding which technique, if any, to implement in order to assimilate SST into their operational hydrodynamic model of the Chesapeake Bay.

1. INTRODUCTION

Temperature is a critical factor in understanding and predicting physical and biological processes in the coastal ocean where they vary considerably in time and space. Physically, its distribution pattern is critical in estimating the density structure and flow. Biologically, several habitat suitability models that have been developed to forecast organisms in the Chesapeake Bay rely on sea-surface temperature (SST) (Constantin de Magny et al. 2009; Jacobs et al. 2014; Urquhart et al. 2014; Hoffman et al. 2012; Brown et al. 2013). Therefore, the ability to measure or estimate temperature synoptically and in near-real time would improve our ability to accurately forecast the physical and biological environment in coastal ocean waters.

Temperature and other physical variables can be predicted by numerical ocean circulation models. Several models of Chesapeake Bay circulation have been developed and refined over the past two decades (Wang and Johnson 2000; Guo and Valle-Levinson 2008; Li et al. 2005, 2006, 2007; Xu et al. 2011; Hoffman et al. 2012). The current operational hydrodynamic model for the Chesapeake Bay of NOAA's National Ocean Service (NOS) —the Chesapeake Bay Operational Forecasting System (CBOFS)—tends to over-predict temperature (relative to observations) throughout the water column. Assimilation of observations into CBOFS has the potential to improve forecasts, however NOAA does not presently assimilate data into the operational forecast systems.

Assimilation of accurate, satellite retrievals of SST into ocean circulation models for shelf and open ocean waters has shown to improve temperature forecasts (Li et al. 2015; Hoffman et al. 2008; Kurapov et al. 2011; Frolov et al., 2009; Chao et al., 2018), but fewer studies have focused on estuarine conditions where physical forcing (e.g. tides, meteorology), estuarine geometry, and bathymetry dominate the dynamics. Some coastal ocean data assimilation studies have used three- (3DVAR) or four-dimensional variational data assimilation (4DVAR) (Yu et al. 2012; Li et al. 2015; Kurapov et al. 2011; Hoteit et al. 2009; Muscarella et al. 2014; Wilkin et al., 2018), while others have used ensemble Kalman filter (EnKF) methods (Hoffman et al. 2008, 2012). In the Chesapeake Bay, Xu et al. (2002) used a nudging method to assimilate two months of salinity data and saw both improvements and disruption of hydrodynamic balance. In addition, Hoffman et al. (2012) used an EnKF method to assimilate simulated satellite SST and *in situ* temperature and salinity observations into a Chesapeake Bay model. Improvements to the temperature field and bias correction were observed, but real data was not used.

In this paper, we use two common data assimilation techniques – Four-Dimensional Variational (4DVAR) assimilation and the Local Ensemble Transform Kalman Filter (LETKF) – to assimilate Suomi National Polar Orbiting Partnership (SNPP) Visible Infrared Imager Radiometer Suite (VIIRS) sea-surface temperature in CBOFS in an effort to provide information about the benefits and costs of assimilating SST into the operational hydrodynamic model of Chesapeake Bay. As such, it is not a rigorous comparison of one technique over another, but a practical exploration of the cost and benefit of adding assimilation to these operational models.

Ensemble Kalman filters and variational methods are the two of the most popular data assimilation methods in use, although recent efforts have focused on developing and implementing hybrid methods that utilize the advantages of both methods (Penny et al. 2015; Lorenc et al. 2014; Wang et al. 2013). While many operational oceanographic systems use 3DVAR (Martin et al. 2015), some have implemented 4DVAR and a hybrid method is applied in a global numerical weather prediction model at NCEP (Penny et al. 2015).

There are a number of differences between variational and EnKF systems and each has its advantages and disadvantages. Studies have compared 4DVAR and LETKF in simple chaotic systems such as the Lorenz 40 variable model and a quasi-geostrophic atmospheric model and have found that both methods have comparable average analysis and forecast errors as long as certain analysis intervals are used (Yang et al. 2009; Fertig et al. 2007). LETKF performance improved with more frequent assimilations while 4DVAR improves with a longer time window (Yang et al. 2009; Fertig et al. 2007). Similar performance has also been seen in more complex models. A comparison between the two methods on the Japanese Operational Atmospheric System also concluded that both systems had similar accuracy, with the LETKF performing better in the northern hemisphere and tropics and 4DVAR performing better in the southern hemisphere (Miyoshi et al. 2010).

In this study, we evaluate implementations of 4DVAR and LETKF in assimilating the satellite retrievals in CBOFS. While many of the comparison studies above compare 4DVAR with 4D-LETKF, here we are using the 4DVAR system that is part of Rutgers University's Regional Ocean Modeling System (ROMS; Haidvogel et al., 2008) and the three-dimensional LETKF. We opt for a three-dimensional LETKF for ease of implementation, speed of computation, and because it has been shown to outperform the 3DVAR systems that are in use operationally for many operational oceanographic systems (Yang et al. 2009; Martin et al. 2015). The ROMS with 3D LETKF for the Chesapeake Bay has been configured and used (Hofmann et al. 2012) and can be readily implemented with CBOFS.

2. DATA AND METHODOLOGY

2.1. Chesapeake Bay Operational Forecast System

The Chesapeake Bay Operational Forecast System (CBOFS) is based on ROMS. The curvilinear, orthogonal horizontal grid employed by the model was generated using the Delft3D-RGFGRID grid generator (http://oss.deltares.nl/documents/183920/185723/RGFGRID_User_Manual.pdf) that allows local grid refinements and seamless pasting of multiple grid segments while still maintaining accurate orthogonality properties. The model domain extends from the 100 m isobath on the shelf at the South to the Susquehanna River reservoir at the North and from Washington, DC at the West to Reedy Point, DE at the East. There are two open ocean boundaries: South – spanning the arc and going up to the 100 m isobath between Ocean City, MD and Duck, NC; East – at Reedy Point, DE along the Chesapeake & Delaware (C & D) Canal. The grid consists of 291 x 332 points in the horizontal and 20 terrain-following vertical levels. The horizontal grid resolution ranges from 34 m to 4895 m and from 29 m to 3380 m in the two (local) coordinate directions. The bathymetry was generated using the NOAA/NOS bathymetric soundings that were interpolated on to the model grid using a local inverse-square interpolation technique.

CBOFS is forced with river, meteorological and open ocean boundary forcing. The river discharges and temperatures are prescribed by the United States Geological Survey (USGS) gauged measurements. The meteorological forcing is applied in CBOFS using the TOGA-COARE Bulk Flux formulation included in ROMS and the forcing physical variables (winds, air temperature, air pressure, air relative humidity, net short-wave radiation flux and downward long wave radiation flux) are provided by the National Weather Service's (NWS) North American Mesoscale (NAM) model at 12 km resolution. At the open boundaries, the purely tidal water level and barotropic currents are prescribed using tidal harmonics from a harmonic constituent database generated at NOAA/NOS/Coast Survey Development Laboratory (CSDL) using the 2-dimensional AdVancedCIRCulation (ADCIRC) model. The sub-tidal water level forcing comes from the NOAA/NWS Extratropic Storm Surge (ETSS) model. For temperature and salinity, the open boundary fields are provided by the Global Real-Time Ocean Forecast System (G-RTOFS) model which is also operated by NOAA/NWS.

The bottom stress is prescribed using the quadratic drag-law formulation and a drag coefficient of 0.005 is employed. The baroclinic time-step used is 10 seconds and a baroclinic:barotropic splitting factor of 20 is prescribed which gives a barotropic time-step of 0.5 s. The operational model is run four times daily and output fields are archived every hour. Variables at discrete station locations are archived every six minutes.

Additional details on the CBOFS model can be found in the Technical Report NOS CS 29 (https://repository.library.noaa.gov/view/noaa/2589).

2.2. Data Assimilation Methodology

2.2.1. 4-Dimensional Variational

When this study was performed, ROMS had three 4DVAR schemes: Incremental Strong Constraint 4DVAR (I4DVAR), Physical Space Statistical Analysis (PSAS), and

Representer 4DVAR (R4DVAR). Moore et al. (2011a) provides a detailed description of each scheme. We selected the I4DVAR scheme, which has been applied in many ROMS data assimilation and ocean prediction systems (Matthews et al. 2012; Zhang et al. 2010a, b; Moore et al. 2011b; Powell et al. 2008; Di Lorenzo et al. 2007). The W4DVAR scheme was not available.

In ROMS, the background and observational covariance matrices are never explicitly formed. Instead, their decomposition matrices or their products with vectors are used in the model calculation. The background covariance matrix is specified using three matrices: the balance operator, the background standard deviation, and the correlation matrix. The observational error covariance is assumed to be diagonal with the specified observational error variance values along the main diagonal.

To compute the standard deviation (of the background), we ran the forward model for one year and calculate the mean and standard deviation of the variables after removing the tidal signal and seasonal cycle. If the tide and annual signals are included, the standard deviation is much larger than that calculated without them. To separate the tides completely from aliasing effects, we re-ran ROMS for six months with the AVERAGES DETIDE option using only 8 major tidal constituents instead of the 37 tidal constituents used in CBOFS (to reduce the file size and computational time while keeping major tidal constituents) imposed along the open boundary. From this, we calculated the tidal harmonics coefficients (tidal phase and amplitude) in the whole ROMS domain from the output tidal file and then use these tidal harmonics coefficients to remove the tidal signal from the model data. The annual cycle was derived using least square fitting of the annual harmonics from the daily averaged dataset of a year-long simulation and interpolated into actual time (every three hours).

To calculate the normalization coefficient for the pseudo-heat algorithm, model error horizontal decorrelation scales must be specified. The horizontal length scales of the SST were estimated using NOAA Advanced Very High Resolution Radiometer (AVHRR) SST data, which are available from NOAA CoastWatch Program (https://coastwatch.noaa.gov) and possess a much longer time series than VIIRS SST. A simple autocorrelation equation was used to calculate the spatial autocorrelation as a function of distance lag. We used the decorrelation scale of 17 km, as estimated in the west-east direction, versus the decorrelation scale of 73 km, as estimated in the north-south direction, as the horizontal decorrelation scale to calculate the normalization coefficient fields in order to prevent over-smoothing of the results. The same length scale was used for the calculation of the normalization coefficient fields for all variables, i.e. temperature, salinity, velocity and surface elevation.

To estimate the vertical decorrelation scale, we viewed 20 years of cruise data across the lower Chesapeake Bay taken by Old Dominion University. It is, however difficult to determine a significant, meaningful decorrelation scale due to the shallow depth of the Bay. Instead, we selected the minimum mixed-layer length, which is 3 m. With the length scales and model grids, ROMS then calculates the normalization matrix for each variable. The multivariate balance between temperature and different variables (such as geostrophic balance, the T-S empirical relations) has been considered in deep ocean ROMS applications. In the Chesapeake Bay, however, salinity largely controls the dynamics, so we did not include the multivariate balance operator in the error covariance normalization. The model dynamics adjusts the other state variables with the assimilation.

The linearization of the tangent linear model from forward model assumes the model state has weak nonlinear evolution in one assimilation window. Given the rapid change of the ocean state with tides in the shallow estuary area, we used an assimilation window of 6 hours, which is approximately half the length of the major tidal period (M2, 12.42 hours) and is the same as the forecasting window of the CBOFS.

2.2.2. Local Ensemble Transform Kalman Filter

Many different flavors of Ensemble Kalman filters exist. In this study we used the LETKF of Hunt et al. (2007). The LETKF has been shown to be an efficient and robust algorithm for atmospheric prediction (Szunyogh et al. 2008; Miyoshi et al. 2010; Miyoshi 2010), forecasting of planetary atmospheres (Hoffman et al. 2010; Greybush et al. 2012), oceanic prediction (Penny et al. 2013), and coastal ocean prediction (Hoffman et al. 2008). The LETKF has also been previously tested with a ROMS model of the Chesapeake Bay in observations system simulation experiments by Hoffman et al. (2012), and this paper uses similar LETKF methodology and a modified version of the code that was used in that study. The code is a modification of open source code published by Takemasa Miyoshi that is freely available (https://github.com/takemasa-miyoshi/letkf) and has been used in many atmospheric studies (Miyoshi and Aranami 2006; Miyoshi and Sato 2007; Miyoshi et al. 2010). While the core of the algorithm is that of the standard LETKF, we discuss changes made to the LETKF workflow specifically for the Chesapeake Bay system as well as the parameters that are used in the LETKF-CBOFS simulations.

Ensemble Forcing and Inflation

Because the Chesapeake Bay is a forced system, errors in the forcing fields have a significant impact on the simulation. If the same wind and river forcing is used for all of the ensemble members, all of the ensemble members tend to converge to the same state, which leads to ensemble collapse and an underestimation of the true background error covariance (Hoffman et al. 2012). This will result in overconfidence in the background estimate, which in turns leads to the system not giving enough weight to new observations.

To combat this, a forcing ensemble was generated by adding in randomly drawn wind perturbations scaled by a specified error perturbation scaling parameter. A scaling factor of 0.4 was used in OSSE experiments and we use that value here (Hoffman et al. 2012). To summarize the process used in Hoffman et al., 2012, a perturbation wind time series is constructed to add to the original wind series. At each forcing time, t, another time t* is randomly selected from within 30 days. The mean wind is subtracted to get the wind anomaly at time t* and this is used to define the wind perturbation. The perturbations are then multiplied by a constant, i.e. 0.4. The forcing perturbation persists for three days, at which point another randomly selected wind field is used for a new perturbation. The procedure is repeated and then smoothed using a 1-day running average. This smoothed perturbation time series is then added to the original wind to create the modified wind forcing. Ideally, the forcing ensemble would be a meteorological forecasting ensemble, which would be more likely to capture the true dynamic uncertainty in the wind. Instead, what is used here is more akin to adding a fraction of error drawn from the normal distribution defined by the climatological error covariance. This is because much of the true error covariance structure is likely determined by the winds. By adding random perturbations to the winds, one is modifying the covariance to reflect the shape created by characteristic winds at other times in addition to the assimilation time, as opposed to only including the dynamic instability.

LETKF Parameters

The forcing ensemble is one way that the ensemble background error covariance is increased to better characterize errors and prevent ensemble collapse. Another way is through covariance inflation. The most commonly used method is multiplicative inflation, where the covariance is multiplied by a parameter with value greater than one. Here we implemented the adaptive inflation method of Takemasa Miyoshi that was previously used by Hoffman et al. (2012) on the Bay. It involves setting an initial inflation value of "1" everywhere in the domain and then letting the system adaptively adjust the inflation at each point (Hoffman et al. 2012).

As with the 4DVAR system, analyses were performed every 6 hr at 00 z, 06 z, 12 z and 18 z using whatever observations were available. A 20-member ensemble was used for the LETKF runs and was initialized by taking states from a model run in August of another year (2012) and re-centering it on the best guess model estimate for 6 August 2014. The choice of ensemble size is a balance between accuracy and computational time. Twenty, which is towards the low end of ensemble size, was chosen based on available computational resources, the relatively high cost of running the model, and experimentation that did not show a large improvement with ensemble of twice the size.

For localization, unit weight is given to observations at the analysis grid point and a Gaussian taper is used to decrease the weight to zero at a distance of $2(\frac{10}{3})^{1/2}\sigma$, where σ is the prescribed Gaussian standard deviation (Gaspari and Cohn 1999). A different σ, with different units in each direction, is used for horizontal and vertical localization due to the nature of the grid. Here we set the horizontal localization as $\sigma = 5$ grid points—which corresponds to a localization radius of approximately 18 grid points—and the vertical localization as $\sigma = 5$ meters—which means corrections are made down to just over 18 meters in the water column. Because the average depth of the Bay is 6 meters, corrections in most locations are made over the entire water column.

2.3. Observations

2.3.1. Visible Infrared Imager Radiometer Suite Sea-Surface Temperature

High resolution (750 m), Level-2 retrievals of sea surface temperature from brightness temperatures measurements collected by the VIIRS onboard the Suomi National Polar Orbiting Partnership (S-NPP) were obtained from NOAA / STAR and data from 08/06/14 to 09/01/14 were assimilated into CBOFS using both techniques. These SST estimates were calculated using NOAA's Advanced Clear-Sky Processor for Oceans (ACSPO) system using heritage regressions with coefficients updated to incorporate the new ACSPO clear- sky and to extend retrievals to the sensors' full swath (Petrenko et al. 2014). The ACSPO corrects for artifacts of bow-tie distortions and striping, as well as for pixel aggregation and pixel deletion (Petrenko et al. 2014; Gladkova et al. 2016). Daytime and Nighttime ACSPO SST are unbiased, with a standard deviation (σ) of 0.466 K and 0.359 K, respectively (Petrenko et al. 2014).

2.3.2. Chesapeake Bay Interpretive Buoy System

In-situ sea surface temperatures of the Chesapeake Bay Interpretive Buoy System (CBIBS) were downloaded from the NOAA Chesapeake Bay Office (http://buoybay.noaa.gov). CBIBS is a network of 11 buoys in the Chesapeake Bay that continuously sample meteorological, oceanographic and water quality conditions, with data available as hourly averages. SST from ten buoys from along the entire length of the Bay were acquired (Fig. 1). The temperature sensor is mounted on the buoy at a depth of 0.5 m.

2.3.3. Chesapeake Bay Program (CBP)

The Chesapeake Bay Program, with support from various funding sources, provides quasi-regular measurements every two to four weeks in the main stem and tributary areas to monitor water quality (Fig. 1). Water temperature profiles were downloaded from the CBP website (http://data.chesapeakebay.net/WaterQuality). The CBP CTD profiles were usually equally spaced with 1 meter interval beginning at 1 m below the surface and ending at 1 m above the bottom.

2.4. Experimental Setup

To compare data assimilation schemes, we ran simulations using both methods starting from initial conditions at 06:00 UTC on 8 August 2014. The initial condition was taken from a CBOFS simulation that was started on 1 January 2014. In addition to the simulations using data assimilation, the uncorrected forward model was run sequentially for the three months of August, September, and October and the model values saved at the observational locations (including CBIBS, CBP and SST locations). The uncorrected forward model is called the freerun and allows a thorough comparison between the models (with/without assimilation of observation) and observations. In both assimilations, the only observations used are satellite SSTs from VIIRS. The CBP and CBIBS observations described above are used for independent validation.

3. RESULTS

Both 4DVAR and LETKF reduce the SST bias errors of the freerun model at all CBIBS stations (Fig. 2). In general, SST bias was corrected throughout the Bay. RMS errors of the freerun model were between 1.19 °C and 2.28 °C and these were reduced to a range of 0.78°C to 1.57°C by the LETKF and 0.71°C to 1.22°C by the 4DVAR system. The smallest improvement was seen in stations close to open boundaries where the SST is controlled by open boundary T/S. For example, the Susquehanna station, which is closest to a river boundary, exhibited the smallest error reduction: 0.06 °C and 0.41 °C by the LETKF and 4DVAR respectively.

Both the LETKF and 4DVAR systems analyses improved the agreement with observations, yet there were clear differences in the two systems. Near the start of the simulation (8/8/14) and after more than three weeks (8/29/14), the LETKF SST field retained most of the features of the model SST, and provided a better match to the assimilated VIIRS observations (Fig. 3). The 4DVAR SST field, on the other hand, exhibited different features in the main stem of the Bay and in the open ocean (Fig. 3).

Even though only surface observations were used, improvements were seen throughout the water column in both the LETKF and 4DVAR assimilations. When compared to the unassimilated CBP temperature profiles from August 2014, the LETKF and 4DVAR systems reduced both RMS error and bias across all vertical levels. Most of this correction appears to be in a bias correction (Fig. 4). While the LETKF did not go far enough in removing the bias, the 4DVAR system overcorrected slightly (Fig. 4). The model bias was 1.67°C for all of the CBP stations, which is reduced to 0.74°C in the LETKF and -0.44°C in the 4DVAR. Similarly, the RMS error was 1.71°C in the free running model, 0.85°C in the LETKF, and 0.59°C in 4DVAR.

Improvements of approximately 1ºC were seen at all depths in profiles from CBP stations CB3.1, CB4.2E, and CB5.4, which are located in the top, middle and lower portions of the Bay, respectively (Fig. 5). The LETKF profiles typically had a similar vertical structure to the model and yielded a much better match with surface observations than at depth (Fig. 5). In the deeper profiles (e.g. Station CB4.2E, Fig. 5, middle panel), the correction was stronger at the surface, which resulted in stronger (temperature) stratification in the LETKF. In shallow regions (e.g. Station CB3.1, Fig. 5, left panel), the model and LETKF profiles shapes are visually similar. The vertical structure of the 4DVAR profiles deviated more from the model, particularly in the shallow parts of the Bay, resulting in a better fit to the observed vertical profiles (Fig. 5, left panel). In deeper stations (e.g. Station CB 5.4), over-corrections near the bottom occurred; this was likely due to unrealistic stratification adjustments (Fig. 5, right panel). Assimilating temperature profiles, in addition to satellite SST observations, may reduce the overcorrections in 4DVAR and improve the vertical structure in LETKF.

Because CBOFS is used for operational forecasts, we also investigated how the improvements from assimilation persist into improving forecasts. Assimilating VIIRS SST significantly improves the forecasting skills over a two-day forecasting window (Fig. 6). The whole model domain averaged SST reduction after data assimilation was clear for both 4DVAR and LETKF (Fig.6 (c)), with a mean initial reduction of SST of 0.80 ºC for LETKF and 1.3ºC for 4DVAR. Along with forecasting time, the forecasting SST from both data assimilation schemes increased towards the freerun SST. The improvement of forecasting skill over the freerun is calculated as:

$$S = 1 - \frac{\sum \quad (F_i^D - O_i)^2}{\sum \quad (F_i^L - O_i)^2}$$

where O_i is the observation (CBIBS) SST at observational time i, F_i^L is the freerun model value at time i, F_i^D is model value (either from 4DVAR or LETKF), and S is the forecasting skill. A model will have a score of 1 for perfect match to observations, a score of 0 for no improvement (the same as freerun results), and negative scores for worse performance than the freerun. Both 4DVAR and LETKF demonstrated improvements of forecasting skills greater than 0.5 for most CBIBS stations. The Susquehanna and Upper Potomac stations have lower values because their locations are too close to either a boundary or a river head where temperatures are prescribed. While forecasting skill decreases with forecasting time, there was still improvement as compared to the freerun in the two-day forecast

While the primary focus was on the impact of SST observation on the temperature field, the 4DVAR assimilation was allowed to correct the salinity field as well using only the VIIRS SST observations. No observations of salinity from CBP or CBIBS were assimilated. Overall, the bias reduction in salinity was small compared to the large salinity bias present in the model (not shown). This is seen in the density profiles of the three stations in Figure 5. The density profiles are essentially unchanged for the LETKF case, and only a small change at some stations, e.g. Station 3.1, for the 4DVAR case. The small correction is likely due to the lack of correlation between temperature and salinity observations, which is why the LETKF was modified to prevent corrections from spurious temperature-salinity correlations. In both systems, the assimilation of *in situ* profiles of salinity is likely to provide the most significant corrections to salinity.

In addition to performance, we also compared the computational cost of LETKF and 4DVAR, especially since the LETKF and 4DVAR simulations were completed on different clusters. The 4DVAR computations were completed on the deepthought2 cluster at the University of Maryland, which uses 2.8 GHz Ivy Bridge Processors while the LETKF computations were completing on the NSF sponsored XSEDE system (Towns et al. 2014) – specifically the Gordon machine – using 2.6 GHz Sandy Bridge processors.

For the results presented here, the LETKF was run using 64 processors and 20 ensemble members while the 4DVAR system used 96 processors and 15 inner loops. In these configurations, it took approximately 6.3 hours for a 6-hour 4DVAR run as compared to 1.25 hours for the LETKF (Table 1). The longer runtime for the 4DVAR is partially caused by reduced efficiency in parallelization for the model beyond 64 processors. We do note that part of the reason for the difference in computation time is due to the difference between taking timing of observations into account for the 4D assimilation (4DVAR) and performing 3D assimilation in the LETKF. Four-dimensional assimilation can be performed with the LETKF as well, and the move from 3D to 4D in the LETKF is expected to be significantly less computationally costly than the current 4D-VAR used here.

In terms of running the algorithms on bigger clusters, the LETKF algorithm can be run in parallel, yet for the relatively low number of observations in the Chesapeake Bay most of the computation time to run the LETKF system is spent running the ensemble forecasts. For the ensemble, the CBOFS model scales reasonably linearly with the number of processors used up to about 64 processors and after that there is slowdown due to the model only partitioning in the horizontal. However, because the LETKF uses ensembles that consist of 20 independent model runs for each 6-hour forecast, the ensemble process is embarrassingly parallel. Thus two or more of the model runs can be done at the same time and the speedup will be almost linear. This means that running two 6-hour forecasts simultaneously on 64 processors each (or possibly 4 on 32 processors each) would be a more efficient—and equally useful—approach than running one forecast at a time on 128 processors. Moreover, each ensemble run can use 64 processors at the same time without message passing, which makes the LETKF method more time efficient compared to the 4DVAR because the total number of CPUs cannot be increased based on inner/outer loop numbers.

4. CONCLUSIONS

Initial comparisons between the 4DVAR and LETKF implementations on the CBOFS model indicate that both techniques provide improvements in sea-surface temperature nowcasts and forecasts over the free running model. The 4DVAR system offers more improvement than the LETKF in reducing SST bias error, especially at depth, but does so at an eightfold increase in computational cost. The performance of 4DVAR over LETKF is not overly surprising because the LETKF implemented here is only three-dimensional.

Both systems improve the temperature simulations throughout the water column using only surface observations, and demonstrates the promise of assimilating remotely sensed SST into CBOFS. We note, however, that the CBP profiles in the test month of August 2014 indicate that there was little thermal stratification in the bay during this time; salinity contributed mostly to the vertical profiles of density during this period. It is unclear how the vertical improvement in both 4DVAR and LETKF would be affected by stratification that can reduce the correlation between surface information and the bottom layers. Observation System Simulation Experiments (OSSEs) on a different ROMS model have indicated that corrections to the bottom in the presence of stratification could lead to incorrect corrections at depth (Hoffman et al., 2012).

The 4DVAR system yielded very small corrections in the salinity field due to the SST observations, which indicates that salinity observations—and most importantly salinity profiles—will be crucial to correcting the salinity bias in the model. While this study assimilates only VIIRS satellite observations, assimilating the *in situ* profiles of both temperature and salinity is possible within the frameworks of both systems and should improve both temperature and salinity nowcasts and forecasts. Even if only satellite SST is assimilated, data assimilation can increase the skill in model predictions of SST and likely other environmental variables in estuaries. Therefore, data assimilation has the potential to improve NOAA’s ability to monitor and predict critical environmental variables in the coastal ocean.

ACKNOWLEDGEMENTS

We thank the Division of Information Technology of the University of Maryland, College Park for providing 260K CPU hours for the 4DVAR computation and NASA Center for Climate Simulation for supplying computer resources for testing of 4DVAR. This work used the Extreme Science and Engineering Discovery Environment (XSEDE), which is supported by National Science Foundation grant number ACI-1053575 for the LETKF computation. Funding for this study was provided by the Joint Polar Satellite System Proving Ground and Risk Reduction Program (NOAA Awards NA09NES4400006, NA14NES4320003) and the Center for Satellite Applications and Research of the National Oceanic and Atmospheric Administration (NOAA). The views, opinions, and findings contained in this report are those of the authors and should not be construed as an official NOAA or U.S. Government position, policy, or decision.

This work was supported by the the National Atmospheric and Oceanic Administration’s Joint Polar Satellite System Proving Ground and Risk Reduction Program under Grants NA09NES4400006 and NA14NES4320003; and by the National Science Foundation under Grant ACI-1053575.

REFERENCES

Brown, C. W., and Coauthors, 2013: Ecological forecasting in Chesapeake Bay: Using a mechanistic–empirical modeling approach. *J. Mar. Syst.*, **125**, 113–125, doi:10.1016/j.jmarsys.2012.12.007.

Chao, Y., J. D. Farrara, H. Zhang, K. J. Armenta, L. Centurioni, F. Chavez, J. B. Girton, D. Rudnick and R. K. Walter, 2018: Development, implementation, and validation of a California coastal ocean modeling, data assimilation, and forecasting system. *Deep Sea Research Part II: Topical Studies in Oceanography*, **151**, 49-63, doi:10.1016/j.dsr2.2017.04.013.

Constantin de Magny, G., W. Long, C. W. Brown, R. R. Hood, A. Huq, R. Murtugudde, and R. R. Colwell, 2009: Predicting the distribution of Vibrio spp. in the Chesapeake Bay: a Vibrio cholerae case study. *EcoHealth*, **6**, 378–389, doi:10.1007/s10393-009-0273-6.

Di Lorenzo, E., A. M. Moore, H. G. Arango, B. D. Cornuelle, A. J. Miller, B. Powell, B. S. Chua, and A. F. Bennett, 2007: Weak and strong constraint data assimilation in the inverse Regional Ocean Modeling System (ROMS): Development and application for a baroclinic coastal upwelling system. *Ocean Model.*, **16**, 160–187, doi:10.1016/j.ocemod.2006.08.002.

Fertig, E. J., J. Harlim, and B. R. Hunt, 2007: A comparative study of 4D-VAR and a 4D Ensemble Kalman Filter: perfect model simulations with Lorenz-96. *Tellus A*, **59**, 96–100, doi:10.1111/j.1600-0870.2006.00205.x.

Frolov, S., A. M. Baptista, T. K. Leen, Z. Lu and R. van der Merwe, 2009: Fast data assimilation using a nonlinear Kalman filter and a model surrogate: An application to the Columbia River estuary. Dynamics of Atmospheres and Oceans, 48(1-3), 16-45. https://doi.org/10.1016/j.dynatmoce.2008.10.004.

Gaspari, G., and S. Cohn, 1999: Construction of correlation functions in two and three dimensions. *Q. J. R. Meteorol. Soc.*, **125**, 723–757.

Gladkova, I., A. Ignatov, F. Shahriar, Y. Kihai, D. Hillger, and B. Petrenko, 2016: Improved VIIRS and MODIS SST Imagery. *Remote Sens.*, **8**, 79, doi:10.3390/rs8010079.

Greybush, S. J., R. J. Wilson, R. N. Hoffman, M. J. Hoffman, T. Miyoshi, K. Ide, T. McConnochie, and E. Kalnay, 2012: Ensemble Kalman filter data assimilation of Thermal Emission Spectrometer temperature retrievals into a Mars GCM. *J. Geophys. Res. Planets*, **117**, E11008, doi:10.1029/2012JE004097.

Guo, X., and A. Valle-Levinson, 2008: Wind effects on the lateral structure of density-driven circulation in Chesapeake Bay. *Cont. Shelf Res.*, **28**, 2450–2471, doi:10.1016/j.csr.2008.06.008.

Haidvogel, D. B., H. Arango, W. P. Budgell, B. D. Cornuelle, E. Curchitser, E. Di Lorenzo, K. Fennel, W. R. Geyer, A. J. Hermann, L. Lanerolle, J. Levin, J. C. McWilliams, A. J. Miller, A. M. Moore, T. M. Powell, A. F. Shchepetkin, C. R. Sherwood, R. P. Signell, J. C. Warner, J. Wilkin, 2008: Ocean forecasting in terrain-following coordinates: Formulation and skill assessment of the Regional Ocean Modeling System, *Journal of Computational Physics*, **227**, 3595-3624, doi: 10.1016/j.jcp.2007.06.016.

Hoffman, M. J., and Coauthors, 2010: An ensemble Kalman filter data assimilation system for the martian atmosphere: Implementation and simulation experiments. *Icarus*, **209**, 470–481, doi:10.1016/j.icarus.2010.03.034.

——, T. Miyoshi, T. W. N. Haine, K. Ide, C. W. Brown, and R. Murtugudde, 2012: An Advanced Data Assimilation System for the Chesapeake Bay: Performance Evaluation. *J. Atmospheric Ocean. Technol.*, **29**, 1542–1557, doi:10.1175/JTECH-D-11-00126.1.

Hoffman, R. N., R. M. Ponte, E. J. Kostelich, A. Blumberg, I. Szunyogh, S. V. Vinogradov, and J. M. Henderson, 2008: A Simulation Study Using a Local Ensemble Transform Kalman Filter for Data Assimilation in New York Harbor. *J. Atmospheric Ocean. Technol.*, **25**, 1638–1656, doi:10.1175/2008JTECHO565.1.

Hoteit, I., B. Cornuelle, S. Y. Kim, G. Forget, A. Köhl, and E. Terrill, 2009: Assessing 4D-VAR for dynamical mapping of coastal high-frequency radar in San Diego. *Dyn. Atmospheres Oceans*, **48**, 175–197, doi:10.1016/j.dynatmoce.2008.11.005.

Hunt, B. R., 2007: Efficient data assimilation for spatiotemporal chaos: A local ensemble transform Kalman filter. *Phys. D*, **230**, 112–126.

Jacobs, J. m., M. Rhodes, C. w. Brown, R. r. Hood, A. Leight, W. Long, and R. Wood, 2014: Modeling and forecasting the distribution of Vibrio vulnificus in Chesapeake Bay. *J. Appl. Microbiol.*, **117**, 1312–1327, doi:10.1111/jam.12624.

Kurapov, A. L., D. Foley, P. T. Strub, G. D. Egbert, and J. S. Allen, 2011: Variational assimilation of satellite observations in a coastal ocean model off Oregon. *J. Geophys. Res. Oceans*, **116**, C05006, doi:10.1029/2010JC006909.

Li, M., L. Zhong, and W. C. Boicourt, 2005: Simulations of Chesapeake Bay estuary: Sensitivity to turbulence mixing parameterizations and comparison with observations. *J. Geophys. Res. Oceans*, **110**, C12004, doi:10.1029/2004JC002585.

——, ——, ——, S. Zhang, and D.-L. Zhang, 2006: Hurricane-induced storm surges, currents and destratification in a semi-enclosed bay. *Geophys. Res. Lett.*, **33**, L02604, doi:10.1029/2005GL024992.

——, ——, ——, ——, and ——, 2007: Hurricane-induced destratification and restratification in a partially-mixed estuary. *J. Mar. Res.*, **65**, 169–192.

Li, Z., J. C. McWilliams, K. Ide, and J. D. Farrara, 2015: Coastal ocean data assimilation using a multi-scale three-dimensional variational scheme. *Ocean Dyn.*, **65**, 1001–1015, doi:10.1007/s10236-015-0850-x.

Lorenc, A. C., N. E. Bowler, A. M. Clayton, S. R. Pring, and D. Fairbairn, 2014: Comparison of Hybrid-4DEnVar and Hybrid-4DVar Data Assimilation Methods for Global NWP. *Mon. Weather Rev.*, **143**, 212–229, doi:10.1175/MWR-D-14-00195.1.

Martin, M. J., and Coauthors, 2015: Status and future of data assimilation in operational oceanography. *J. Oper. Oceanogr.*, **8**, s28–s48, doi:10.1080/1755876X.2015.1022055.

Matthews, D., B. S. Powell, and I. Janeković, 2012: Analysis of four-dimensional variational state estimation of the Hawaiian waters. *J. Geophys. Res. Oceans*, **117**, C03013, doi:10.1029/2011JC007575.

Miyoshi, T., 2010: The Gaussian Approach to Adaptive Covariance Inflation and Its Implementation with the Local Ensemble Transform Kalman Filter. *Mon. Weather Rev.*, **139**, 1519–1535, doi:10.1175/2010MWR3570.1.

——, and K. Aranami, 2006: Applying a Four-dimensional Local Ensemble Transform Kalman Filter (4D-LETKF) to the JMA Nonhydrostatic Model (NHM). *Sola*, **2**, 128–131, doi:10.2151/sola.2006-033.

——, and Y. Sato, 2007: Assimilating Satellite Radiances with a Local Ensemble Transform Kalman Filter (LETKF) Applied to the JMA Global Model (GSM). *Sola*, **3**, 37–40, doi:10.2151/sola.2007-010.

——, ——, and T. Kadowaki, 2010: Ensemble Kalman Filter and 4D-Var Intercomparison with the Japanese Operational Global Analysis and Prediction System. *Mon. Weather Rev.*, **138**, 2846–2866, doi:10.1175/2010MWR3209.1.

Moore, A. M., and Coauthors, 2011a: The Regional Ocean Modeling System (ROMS) 4-dimensional variational data assimilation systems: Part III – Observation impact and observation sensitivity in the California Current System. *Prog. Oceanogr.*, **91**, 74–94, doi:10.1016/j.pocean.2011.05.005.

——, H. G. Arango, G. Broquet, B. S. Powell, A. T. Weaver, and J. Zavala-Garay, 2011b: The Regional Ocean Modeling System (ROMS) 4-dimensional variational data assimilation systems: Part I – System overview and formulation. *Prog. Oceanogr.*, **91**, 34–49, doi:10.1016/j.pocean.2011.05.004.

Muscarella, P. A., M. J. Carrier, and H. E. Ngodock, 2014: An examination of a multi-scale three-dimensional variational data assimilation scheme in the Kuroshio

Extension using the naval coastal ocean model. *Cont. Shelf Res.*, **73**, 41–48, doi:10.1016/j.csr.2013.11.009.

Penny, S. G., E. Kalnay, J. A. Carton, B. R. Hunt, K. Ide, T. Miyoshi, and G. A. Chepurin, 2013: The local ensemble transform Kalman filter and the running-in-place algorithm applied to a global ocean general circulation model. *Nonlin Process. Geophys*, **20**, 1031–1046, doi:10.5194/npg-20-1031-2013.

Penny, S. G., D. W. Behringer, J. A. Carton, and E. Kalnay, 2015: A Hybrid Global Ocean Data Assimilation System at NCEP. *Mon. Weather Rev.*, **143**, 4660–4677, doi:10.1175/MWR-D-14-00376.1.

Petrenko, B., A. Ignatov, Y. Kihai, J. Stroup, and P. Dash, 2014: Evaluation and selection of SST regression algorithms for JPSS VIIRS. *J. Geophys. Res. Atmospheres*, **119**, 2013JD020637, doi:10.1002/2013JD020637.

Powell, B. S., H. G. Arango, A. M. Moore, E. Di Lorenzo, R. F. Milliff, and D. Foley, 2008: 4DVAR data assimilation in the Intra-Americas Sea with the Regional Ocean Modeling System (ROMS). *Ocean Model.*, **23**, 130–145, doi:10.1016/j.ocemod.2008.04.008.

Frolov, S., A. M. Baptista, T. K. Leen, Z. Lu and R. van der Merwe, 2009: Fast data assimilation using a nonlinear Kalman filter and a model surrogate: An application to the Columbia River estuary. *Dynamics of Atmospheres and Oceans*, 48(1-3), 16-45, doi: 10.1016/j.dynatmoce.2008.10.004.

Szunyogh, I., E. J. Kostelich, G. Gyarmati, E. Kalnay, B. R. Hunt, E. Ott, E. Satterfield, and J. A. Yorke, 2008: A local ensemble transform Kalman filter data assimilation system for the NCEP global model. *Tellus A*, **60**, 113–130, doi:10.1111/j.1600-0870.2007.00274.x.

Towns, J., and Coauthors, 2014: XSEDE: Accelerating Scientific Discovery. *Comput. Sci. Eng.*, **16**, 62–74, doi:10.1109/MCSE.2014.80.

Urquhart, E. A., B. F. Zaitchik, D. W. Waugh, S. D. Guikema, and C. E. Del Castillo, 2014: Uncertainty in Model Predictions of Vibrio vulnificus Response to Climate Variability and Change: A Chesapeake Bay Case Study. *PLoS ONE*, **9**, e98256, doi:10.1371/journal.pone.0098256.

Wang, H. V., and B. H. Johnson, 2000: Validation and Application of the Second Generation Three Dimensional Hydrodynamic Model of Chesapeake Bay. *Water Qual. Ecosyst. Model.*, **1**, 51–90, doi:10.1023/A:1013982515467.

Wang, X., D. Parrish, D. Kleist, and J. Whitaker, 2013: GSI 3DVar-Based Ensemble–Variational Hybrid Data Assimilation for NCEP Global Forecast System: Single-Resolution Experiments. *Mon. Weather Rev.*, **141**, 4098–4117, doi:10.1175/MWR-D-12-00141.1.

Wilkin, J., J. Levin, A. Lopez, E. Hunter, J. Zavala-Garay, Javier, and H. Arango. 2018. A Coastal Ocean Forecast System for U.S. Mid-Atlantic Bight and Gulf of Maine. 10.17125/gov2018.ch21.

Xu, J., S.-Y. Chao, R. R. Hood, H. V. Wang, and W. C. Boicourt, 2002: Assimilating high-resolution salinity data into a model of a partially mixed estuary. *J. Geophys. Res. Oceans*, **107**, 11–1, doi:10.1029/2000JC000626.

——, W. Long, J. D. Wiggert, L. W. J. Lanerolle, C. W. Brown, R. Murtugudde, and R. R. Hood, 2011: Climate Forcing and Salinity Variability in Chesapeake Bay, USA. *Estuaries Coasts*, **35**, 237–261, doi:10.1007/s12237-011-9423-5.

Yang, S.-C., M. Corazza, A. Carrassi, E. Kalnay, and T. Miyoshi, 2009: Comparison of Local Ensemble Transform Kalman Filter, 3DVAR, and 4DVAR in a Quasigeostrophic Model. *Mon. Weather Rev.*, **137**, 693–709, doi:10.1175/2008MWR2396.1.

Yu, P., A. L. Kurapov, G. D. Egbert, J. S. Allen, and P. M. Kosro, 2012: Variational assimilation of HF radar surface currents in a coastal ocean model off Oregon. *Ocean Model.*, **49**–**50**, 86–104, doi:10.1016/j.ocemod.2012.03.001.

Zhang, W. G., J. L. Wilkin, and H. G. Arango, 2010a: Towards an integrated observation and modeling system in the New York Bight using variational methods. Part I: 4DVAR data assimilation. *Ocean Model.*, **35**, 119–133, doi:10.1016/j.ocemod.2010.08.003.

——, ——, and J. C. Levin, 2010b: Towards an integrated observation and modeling system in the New York Bight using variational methods. Part II: Repressenter-based observing strategy evaluation. *Ocean Model.*, **35**, 134–145, doi:10.1016/j.ocemod.2010.06.006.

APPENDIX A: TABLES

Table 1. Computational load for 4DVAR and LETKF

DA Method	Processors	Time to Run 6 Hours	Time for One 2.8 GHz CPU	Notes
I4DVAR	96 (2.8 GHz)	~6.3 Hours	~604 Hours	15 Inner Loops / 1 Outer Loop
LETKF	64 (2.6 GHz)	~1.25 Hours	75 Hours (No CPU Scaling)	20 Ensemble Members

APPENDIX B: FIGURES

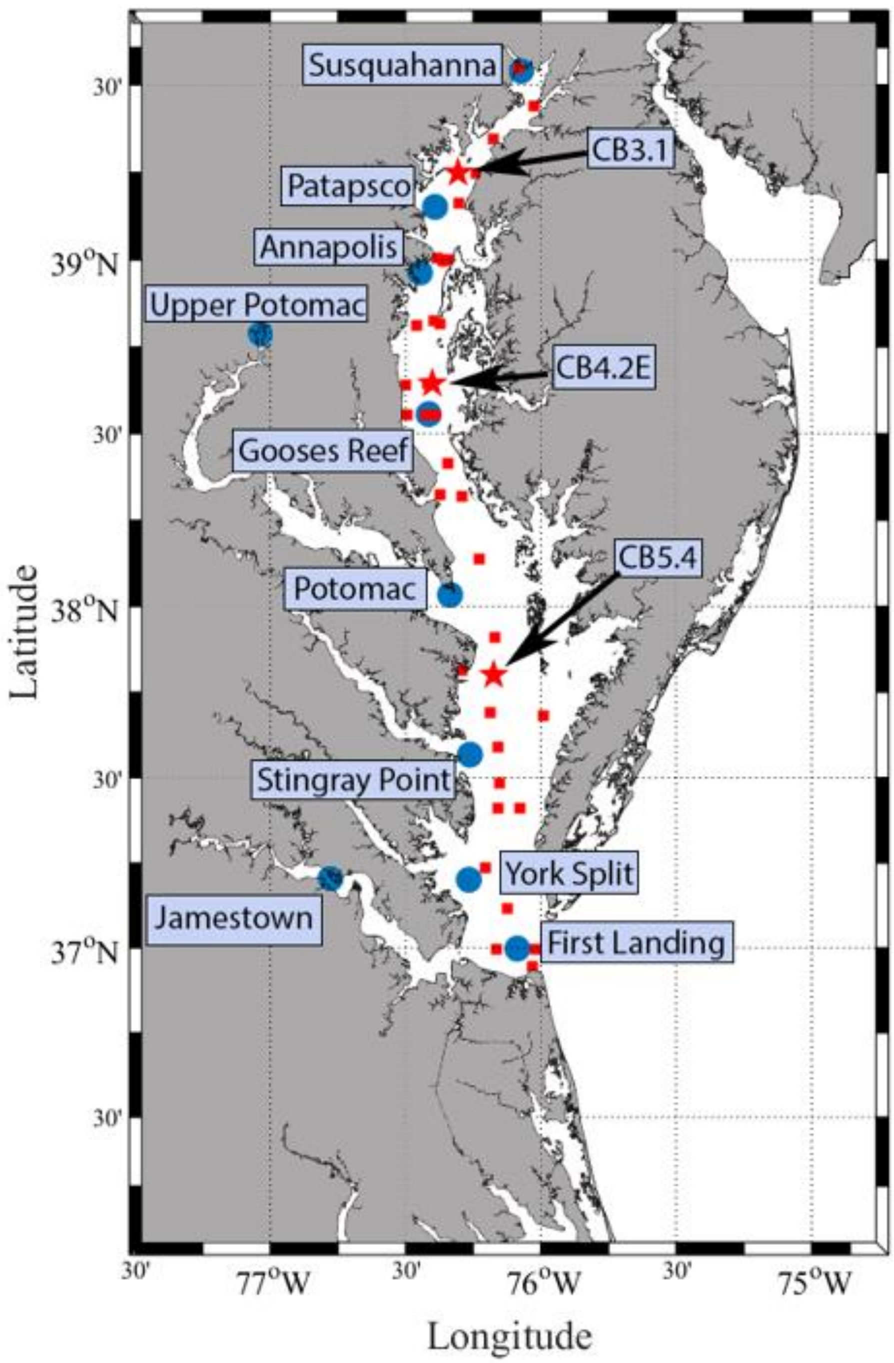

Figure 1. Buoy locations of the Chesapeake Bay Interpretive Buoy System (CBIBS; blue circles), whose observations were used in evaluating satellite retrievals and hydrodynamic model predictions of sea surface temperature, and the Chesapeake Bay Program (CBP; red squares and stars), whose vertical profiles were used in the evaluation of the assimilation results. The labeled red stars are the locations of stations shown in Figure 5.

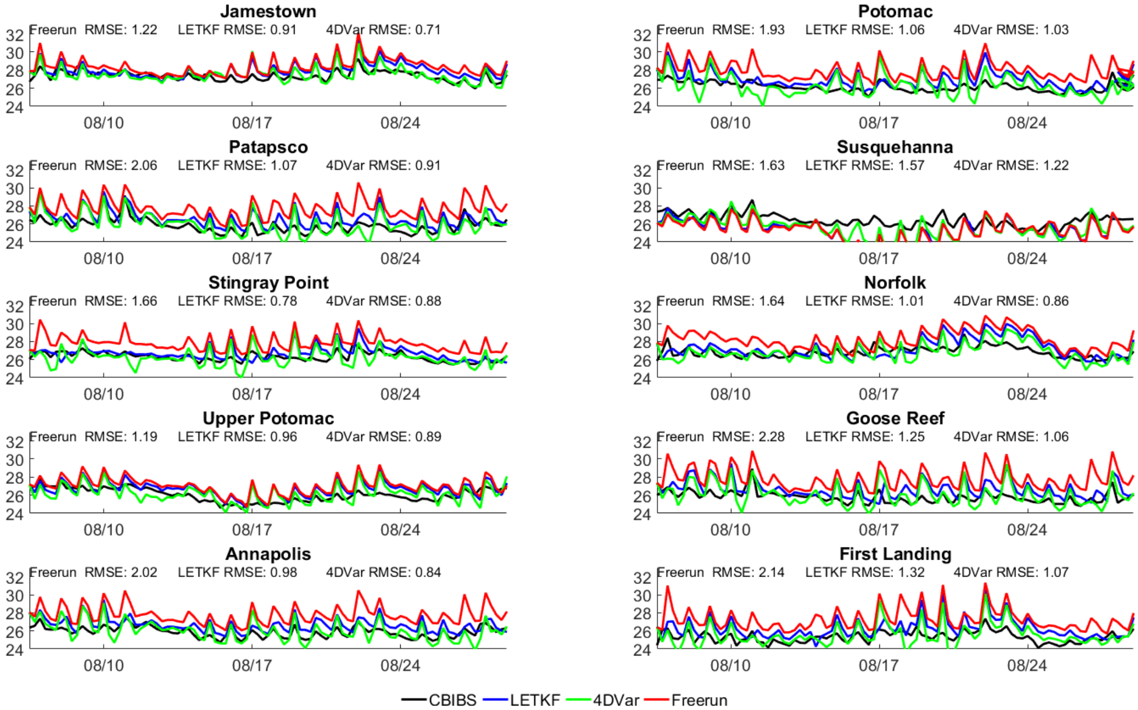

Figure 2. Comparison of 4DVAR (green), LETKF (blue), and freerunning model (red) sea surface temperature (°C) results with observations from the study period at the CBIBS stations (black) shown in Figure 1.

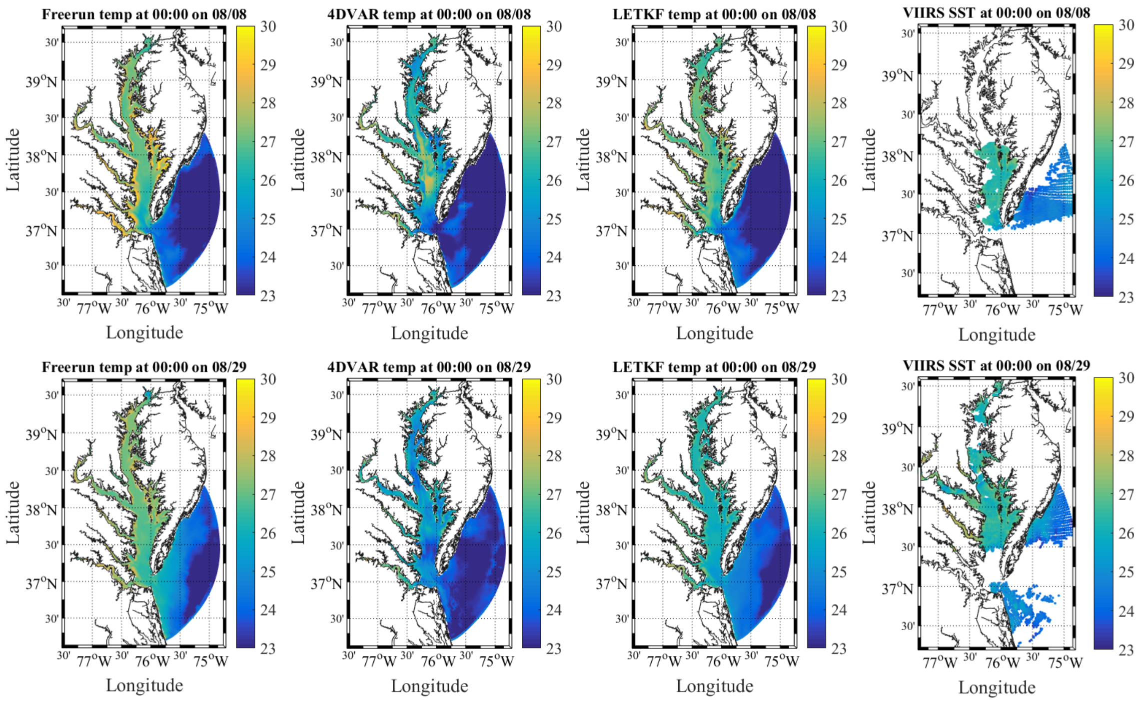

Figure 3. Comparison of sea surface temperature (°C) fields from the model, 4DVAR, LETKF, and VIIRS on August 8, 2014 (top row; near the start of the simulation) and August 29, 2014 (bottom row; near the end of the simulation). Differences are apparent through the main stem of the Bay.

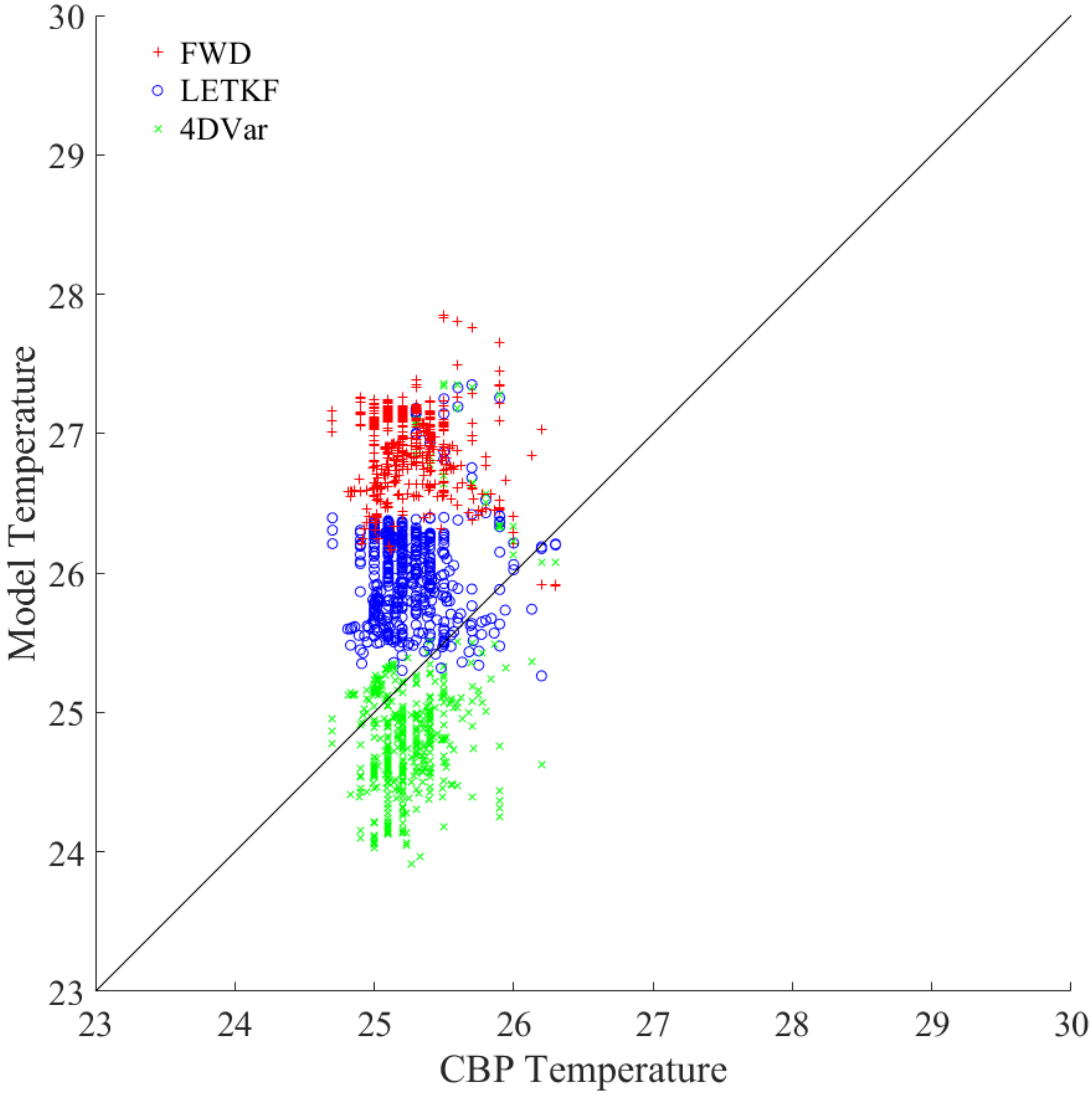

Figure 4. Comparison of 4DVAR (green) and LETKF (blue) analysis results and the freerun model (red) with all available CBP station temperature (°C) data from August 6 to August 31, 2014. The comparison includes temperatures from all vertical levels and shows that most of the error in the freerun model is a warm bias. Both the 4DVAR and LETKF remove much of this bias.

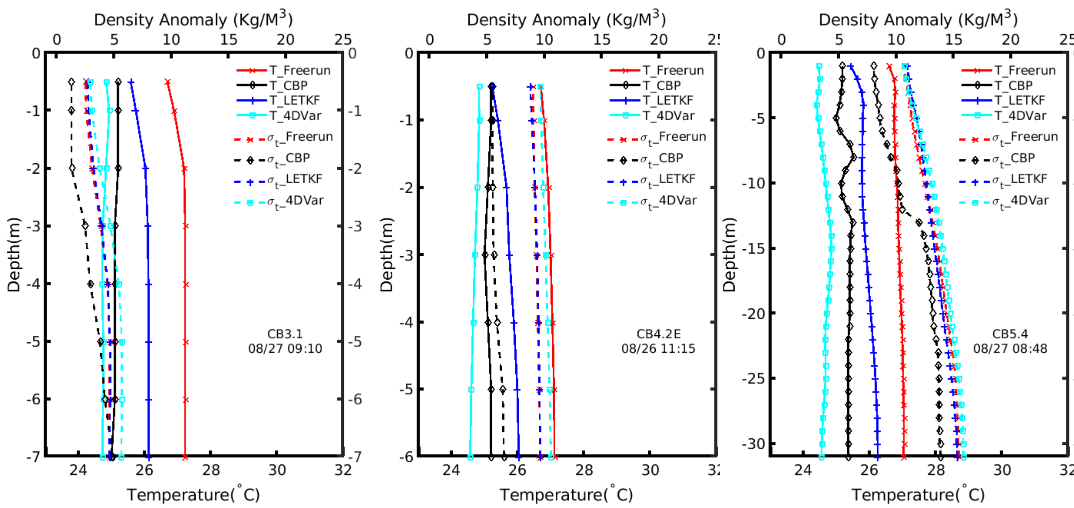

Figure 5. Comparison of 4DVAR, LETKF, and freerun model temperature (°C) (solid line) and density anomaly profiles (dashed line) with independent observations at three CBP stations (black). The CBP stations are shown as stars in Fig. 1. The density anomaly is referenced to 1000 kg/m^3. The warm bias of the model is apparent and the correction in both LETKF and 4DVAR occurs at all levels, even though only sea surface temperature is assimilated. The 4DVAR temperature profile changes while the LETKF profile mirrors the model.

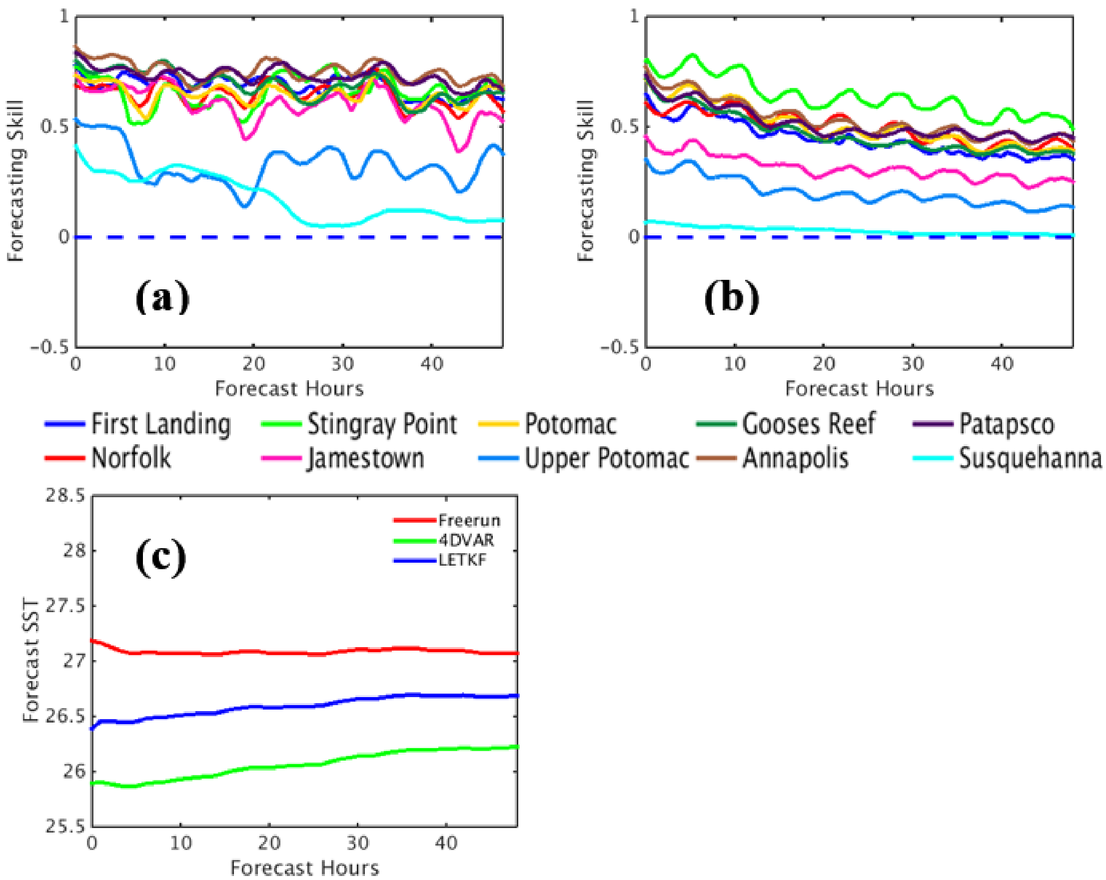

Figure 6. Forecasting skills over 48 hours with assimilation of S-NPP VIIRS SST using (a) 4DVAR and (b) LETKF data assimilation at the 10 CBIBS stations, and whole model domain averaged SST (c). The freerun forecast is defined as zero (blue dashed line). Both techniques reduce SST immediately, yet rise gradually with forecasting time without continued assimilation. Note that the VIIRS SST observational mean during the assimilation period is about 25.8 °C.